JOURNAL OF MOLECULAR SPECTROSCOPY 160, 192–216 (1993)

The Pattern of Clusters in Isolated Vibrational Components of CF_4 and the Semiclassical Model

B. I. ZHILINSKII,[1] SVEND BRODERSEN,[2] AND MORTEN MADSEN

Department of Chemistry, Aarhus University, Langelandsgade 140, DK-8000 Aarhus C, Denmark

The semiclassical model for the rotation of molecules is used to interpret the rotation–vibrational energy level diagram of CF_4. The definition of the model is sharpened, partly by means of the splitting of the energy levels into vibrational components and partly by introducing limitations in the possible shapes of the classical rotational energy surface. The model is used to discuss the pattern of clusters in each manifold of energy levels. The appearance of clusters in series of 6-fold, 8-fold, 12-fold, and 24-fold clusters is explained. It is also shown that folded series are a simple consequence of the model. The pattern of clusters in isolated vibrational components as a function of J is discussed with special attention to a rather common reversal of the pattern of clusters. On the basis of the possible qualitative changes in the shape of the rotational surface, these reversals are shown to appear only in two types, the simple inversion and the complex inversion. By means of examples, the details of both kinds of inversion are shown to be in full agreement with the qualitative requirements of the model. Finally, a quantitative application of the model to the vibrational ground state is presented.

INTRODUCTION

Heavy spherical top molecules are of special spectroscopic interest because of a pronounced tendency for these molecules to form clusters of rotation–vibration states. The best studied molecule of this type is CF_4, which offers a wealth of examples of such clusters. Also, the potential function of this molecule is known rather accurately, making possible a calculation of both the energies and the wavefunctions, which are essential in understanding the different patterns of clusters.

The potential function of CF_4 has been fitted to the experimental transition frequencies, and using a polynomial expansion including all 51 terms up to the fourth degree in the symmetry coordinates, a very close agreement with the spectroscopic data has been obtained (*1, 2*). This potential has been used to compute the energies and wavefunctions of a very large number of rotation–vibration states (*3*). The following 10 vibrational states were included: the ground state, all 4 fundamental states, $\nu_1 + \nu_2$, $2\nu_2$, $3\nu_2$, $2\nu_4$, and $\nu_2 + \nu_4$. The overall vibrational degeneracy of all these states is 31. The energies have been computed for all $J \leqslant 70$, whereas the wavefunctions have been calculated for all $J \leqslant 50$, and in some cases for $J \leqslant 70$. The calculations have been performed for all three isotopic species of CF_4. On the basis of these wavefunctions, it has been possible to define a *cluster index* $\tau = 0, 1, 2, \ldots$ for any cluster, and it has been shown that all the states may be divided between 31 *vibrational components*, corresponding to a complete removal of the vibrational degeneracy (*3*). The use of these two concepts allows a substantial ordering of all the vibration–rotation states. The basic unit of this ordering is one *manifold*, which in the present paper

[1] On leave of absence from Department of Chemistry, Moscow State University, Moscow 119899.

[2] Author to whom correspondence should be addressed.

0022-2852/93 $5.00

means the collection of vibration–rotation states within one vibrational component for one value of J. The clusters appearing within one such manifold can always be arranged in one series of 6-fold clusters and one series of 8-fold clusters, and more rarely also a series of 12-fold clusters; the cluster index in all cases varies from zero to some maximum value. Also, 24-fold clusters appear, as discussed below.

The 31 vibrational components of the three isotopic species consist of about 6500 manifolds. It is clearly difficult to obtain a survey of the pattern of clusters within all these manifolds without some kind of systematization. It has already been shown (*3*) that the pattern of clusters within more than half of these manifolds follows one of two schemes, termed type I and type II, but many other schemes appear, and it seems difficult immediately to find a general principle for an ordering. The scope of the present paper is to present a procedure for finding what pattern of clusters may appear and why they appear in different cases. The basis of this procedure is a comparison to the semiclassical model for the rotation of spherical top molecules, consisting mainly of a definition of a classical rotational energy surface for each manifold and certain approximate quantization conditions. This model has been used extensively by Harter and Patterson (*4, 5, 6*) to treat some cases of the pattern of clusters on the basis of simple operators and by Zhilinskii *et al.* (*7, 8, 9, 10*) for more realistic rovibrational Hamiltonians. In the present paper the definition of this model is sharpened considerably and the different possibilities for the patterns of clusters are presented on the basis of a search for the possible shapes of the rotational energy surface and the possible changes between such shapes. These possibilities are compared to the patterns of the computed clusters, and a very nice agreement is found.

THE SEMICLASSICAL MODEL

Definition of the Rotational Energy Surface

The classical rotational energy E of a molecule rotating in a field-free space is given as

$$E = \frac{P_a^2}{2I_a} + \frac{P_b^2}{2I_b} + \frac{P_c^2}{2I_c}, \tag{1}$$

where P_a, P_b, and P_c are the components of the angular momentum $\mathbf{P}$ on the principal axis of the molecule, and I_a, I_b, and I_c are the corresponding principal moments of inertia. The angular momentum may instead be characterized by $|\mathbf{P}|$ and two angles ϑ and φ indicating the direction of $\mathbf{P}$ in a molecule-fixed coordinate system. The classical energy then becomes a function of $|\mathbf{P}|$, ϑ, φ, and the three principal moments of inertia. The moments of inertia vary with the rotation (as described by $\mathbf{P}$) and with the vibration of the molecule.

We want to define a rotational energy surface for each manifold of rotation–vibration states in the sense defined above. It seems safe to assume that the vibrational influence on the moments of inertia is constant for one such manifold, so that the three moments of inertia are functions of $\mathbf{P}$ only. When J is constant, $|\mathbf{P}|$ is also a constant, and the classical energy is a function of ϑ and φ only. Consequently, the rotational energy surface corresponding to one manifold of states is defined as the surface illustrating the classical energy E as a function of ϑ and φ for the constant value of $|\mathbf{P}|$. This surface is almost a sphere, because the three principal moments of inertia are always nearly equal for a spherical top molecule. In fact, the deviation from a perfect sphere

is never more than 3 cm^{-1} for CF_4 if $J \leq 70$, and is often much smaller. It is, however, these small deviations which make the surface interesting.

The Shape of the Rotational Energy Surface

The rotational energy surface has some important symmetry properties. The value of E is the same for two opposite directions of $\mathbf{P}$ when $|\mathbf{P}|$ is constant, and the surface must have a center of symmetry i. It may be shown (*11, 12*) that the surface always has the symmetry of $T_d \otimes i = O_h$, even if the molecule has lost some of its symmetry because of centrifugal and vibrational distortions of the geometry.

The O_h point group contains three C_4 axes (coincident with the S_4 axes of the molecule), four C_3 axes, and six C_2 axes (perpendicular to the σ_d symmetry planes of the molecule). The points where these axes cut the surface are of special importance, and we call them the C_4, the C_3, and the C_2 points, respectively. There are thus 6 C_4 points, 8 C_3 points, and 12 C_2 points on each surface. These numbers are closely related to the appearance of 6-fold, 8-fold, and 12-fold clusters, respectively, as discussed below.

Because of the high symmetry it is easily seen that the surface may be divided into 48 spherical triangles which are either identical or mirror images of each other. In order to describe the detailed form of the surface it is sufficient to describe one of these triangles. The vertices of such a triangle are one C_4 point, one C_3 point, and one C_2 point (see Fig. 1). The side of the triangle from the C_4 point to the C_2 point is defined by a σ_h symmetry plane of the O_h point group, whereas the other two sides both are defined by the σ_d symmetry planes (*11, 10*). Any point on one of these sides

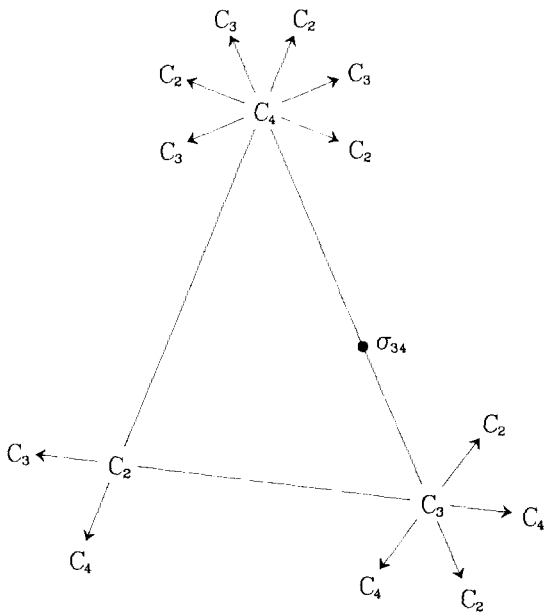

FIG. 1. One of the 48 equivalent spherical triangles on the classical rotational energy surface. The arrows indicate the directions to the vertices of the neighboring triangles. As an example, the position of a set of σ_{34} points are included. Due to the problems in reproducing a spherical triangle as a plane figure, the angles at the C_2 point are unfortunately not 90°.

is symmetrically equivalent to 23 other points. We shall refer to each of these 24 equivalent points on the surface as σ_{23}, σ_{24}, or σ_{34} points, where the two indices indicate the order of the two axes at the corresponding vertices. Thus, a σ_{34} point is one of the 24 points lying at the intersection between the rotational energy surface and one of the σ_d planes defined by a C_3 and a C_4 axis (see Fig. 1). We refer to all three kinds of such points as σ points. Finally, we use the term C_1 for any member of a set of 48 points inside the triangle.

In order to get more detailed information on the possible shapes of the surface we use the general theory of surfaces, in which maxima, minima, and saddle points are termed stationary points. These stationary points may be either degenerate or nondegenerate, depending on the eigenvalues of the 2×2 Hessian matrix formed by the second derivatives of the energy taken at that point. If any of these eigenvalues is zero, the stationary point is degenerate, because a small change, for instance in the potential function, may change, say, a maximum into a saddle point or a minimum. This would be an unacceptable situation when describing a stable situation of the molecule, and we define as an essential part of the model that all stationary points on the rotational energy surface must be nondegenerate, which means that both the eigenvalues of the Hessian matrix must be nonzero. However, in the description of the transformations between stable situations, we allow degenerate stationary points to appear, as discussed in the following section.

Functions with only nondegenerate stationary points are named Morse-type functions (*13, 11, 14, 15*). If, as in the present case, they are functions of two spherical coordinates only, there exist the Euler relation

$$n_{\max} + n_{\min} = n_{\text{sad}} + 2, \tag{2}$$

where $n_{\max}$ is the number of maxima, etc., and the Morse inequalities

$$n_{\text{sad}} + 1 \geqslant n_{\min} \geqslant 1. \tag{3}$$

Because of the presence of the symmetry axis, the tangential plane of the surface in any C_4 or C_3 point is necessarily perpendicular to the axis (coincident with the radius of that point), and the surface must have either a maximum or a minimum in any of these points, and because of the symmetrical equivalence the same type in all 6 or 8 points of the same kind. Thus, if, for instance, the surface has a maximum at one of the C_4 points, it necessarily has a maximum at all 6 C_4 points. At the 12 C_2 points it is possible to have a maximum, a minimum, or a saddle point (with a maximum in one section, but a minimum in another section). Finally, at the 24 σ points and at the 48 C_1 points there may be a maximum, a minimum, a saddle point, or just a slope. In connection with this information, Eqs. (2) and (3) lead to important restrictions on the possible combinations of minima, maxima, and saddle points on the rotational energy surface.

If we first assume that only the C_4, C_3, and C_2 points are stationary (as they must be), it is easy to see that there are only two possible shapes of the surface. If there are minima at the C_4 points, there must be maxima at the C_3 points and saddle points at the C_2 points. If there are maxima at the C_4 points, there must be minima at the C_3 points and saddle points at the C_2 points. At all other points of the surface, there is just a slope in both cases. These two shapes are indicated as Nos. 1 and 2 in Table I. Below we show that they lead to the type I and type II patterns of clusters mentioned in the introduction.

TABLE I

Shapes of the Rotational Energy Surface

No.	Equivalent sets of points						Pattern of clusters
	$6C_4$	$8C_3$	$12C_2$	$24\sigma_{24}$	$24\sigma_{34}$	$24\sigma_{23}$	
1	min	max	saddle				6- and 8-fold clusters, type I
2	max	min	saddle				6- and 8-fold clusters, type II
3	min	max	max			saddle	6-, 8-, and 12-fold clusters
4	min	min	max		saddle		6-, 8-, and 12-fold clusters
5	max	min	max	saddle			6-, 8-, and 12-fold clusters
6	min	max	min	saddle			6-, 8-, and 12-fold clusters
7	max	max	min		saddle		6-, 8-, and 12-fold clusters
8	max	min	min			saddle	6-, 8-, and 12-fold clusters
9	min	min	saddle	max	saddle		6-, 8-, and 24-fold clusters or
10	min	min	saddle	saddle	max		folded series
	–	–	–	–	–		
27	min	min	min	saddle	max	saddle	6-, 8-, and 24-fold clusters or
	–	–	–	–	–		folded series

Next, if one set of σ points is allowed to be stationary, 6 different shapes are possible, given as Nos. 3 to 8 in Table I. Here is further utilized the obvious rule that a saddle point must be present on the one side of the triangle connecting either two maxima or two minima. The next step is to allow two sets of σ points to be stationary, resulting in 18 different shapes of the surface. Out of these, only two are included in Table I as examples. These two possibilities have been chosen because they appear in practice in one of the components of the ν_2 state, as discussed in detail below. There is an increasing number of possible shapes the more sets of stationary points that are allowed, and Table I should thus in principle be infinitely long.

The Shape of the Rotational Energy Surface as a Function of J

Below we correlate the variation with J of the pattern of clusters within one vibrational component with the changes in the shape of the rotational surface as a function of J. In the present section we indicate what changes are possible in the rotational surface due to variations in J (*16*). Such changes are of three different kinds. First, the surface may change quantitatively without any change in the position of maxima, minima, or saddle points. Second, the position of, say, a maximum at any set of 24 σ points, may vary continuously along one side of the triangle, or the position of a minimum at some set of C_1 points may change inside the triangle. These positions are not determined by symmetry, and such a change is again a quantitative change. Third, new maxima, minima, or saddle points may turn up or they may disappear. This is a qualitative change in the shape of the surface, and therefore such changes are of special importance.

Any qualitative change in the shape of the rotational surface goes through a transition state in which each member of one set of symmetrically equivalent points becomes a degenerate stationary point. This is best seen by means of an example. Let us assume that the rotational surface (besides other stationary points) has one set of 24 maxima at some σ point and another set of 24 saddle points at some other σ point very close

by. If these two sets of stationary points move towards each other due to an increase in J, they will coalesce into one set of degenerate stationary points. As stated above, this corresponds to a physically unstable situation which should be considered as an unobservable transition state. The degenerate stationary point will immediately transform into a nonstationary point, which means that the maxima and saddle points have annihilated each other, leaving just an ordinary sloped surface at the actual position.

This change in the shape of the rotational surface is indicated in line No. 11 of Table II, if read from right to left. It is immediately clear that the reverse change is also possible, creating close to any set of σ points, one set of 24 maxima and simultaneously a set of 24 saddle points. But two further changes of this kind are possible, in which 24 minima are involved instead of the 24 maxima. Thus, line No. 11 of Table II indicates the possibility of four closely related qualitative changes in the shape of the rotational surface. The important point is that only 48 different qualitative changes are possible due to a change of J, as listed by the 12 lines of Table II, where each line indicates four changes, obtained by reading both ways and by replacing maxima by minima and minima by maxima. For each line of Table II the set of intermediate degenerate stationary points is indicated in the last column.

A few more examples will illustrate the use of Table II.

Line No. 5 states that 12 maxima at the C_2 positions may change into 12 saddle points, if simultaneously a set of 24 new maxima are formed at some σ_{23} points very close to the C_2 points. This means that each C_2 maximum is transformed into a saddle point and two close-lying new maxima.

Line No. 4 indicates that if maxima exist at all 8 C_3 points and each of these are surrounded by three neighboring σ_{23} saddle points, these three saddle points may pass through the C_3 point and become three σ_{34} saddle points, changing the C_3 maximum into a minimum. Such a passage of three saddle points for each C_3 point is the

TABLE II

All Possible Qualitative Changes in the Shape of the Rotational Energy Surface Due to Variations in J

No.	Change	Deg. stat. point
1	$6\,C_4$ max. $\leftrightarrow$ $6\,C_4$ min. + $24\,\sigma_{24}$ sad. + $24\,\sigma_{34}$ max.	C_4
2	$6\,C_4$ max. $\leftrightarrow$ $6\,C_4$ min. + $24\,\sigma_{34}$ sad. + $24\,\sigma_{24}$ max.	C_4
3	$6\,C_4$ max. + $24\,\sigma_{34}$ sad. $\leftrightarrow$ $6\,C_4$ min. + $24\,\sigma_{24}$ sad.	C_4
4	$8\,C_3$ max. + $24\,\sigma_{23}$ sad. $\leftrightarrow$ $8\,C_3$ min. + $24\,\sigma_{34}$ sad.	C_3
5	$12\,C_2$ max. $\leftrightarrow$ $12\,C_2$ sad. + $24\,\sigma_{23}$ max.	C_2
6	$12\,C_2$ max. $\leftrightarrow$ $12\,C_2$ sad. + $24\,\sigma_{24}$ max.	C_2
7	$12\,C_2$ sad. $\leftrightarrow$ $12\,C_2$ max. + $24\,\sigma_{23}$ sad.	C_2
8	$12\,C_2$ sad. $\leftrightarrow$ $12\,C_2$ max. + $24\,\sigma_{24}$ sad.	C_2
9	$24\,\sigma_{ij}$ max. $\leftrightarrow$ $24\,\sigma_{ij}$ sad. + $48\,C_1$ max.	σ_{ij}
10	$24\,\sigma_{ij}$ sad. $\leftrightarrow$ $24\,\sigma_{ij}$ max. + $48\,C_1$ sad.	σ_{ij}
11	slope $\leftrightarrow$ $24\,\sigma_{ij}$ max. + $24\,\sigma_{ij}$ sad.	σ_{ij}
12	slope $\leftrightarrow$ $48\,C_1$ max. + $48\,C_1$ sad.	C_1

Each line indicates four possible changes obtained by reading both ways and by replacing maxima by minima and minima by maxima.

only way in which the maxima at the C_3 positions may be changed into minima or vice versa.

Six maxima at the C_4 points may also be changed into minima, as indicated in line No. 3, by means of a passage of saddle points. But for the C_4 points there is one further possibility given in line Nos. 1 and 2. The six C_4 maxima may be changed into minima if a set of 24 σ_{34} (or σ_{24}) maxima and a set of 24 σ_{24} (or σ_{34}) saddle points are formed simultaneously at neighboring positions. After this transformation each C_4 minimum is surrounded by four maxima and four saddle points, forming a rim around the minimum.

The most important information given by Table II is that several qualitative changes of the surface are impossible as the result of a variation of J in the present model. Thus a set of maxima cannot just change into minima. Such a change must always be accompanied by some other qualitative changes. This has very important consequences for the possible changes in the pattern of clusters within one vibrational component as the result of a change in J, as discussed in detail below.

The Quantization Condition

The most common shape of the rotational energy surface is the one indicated as No. 1 in Table I. It has 8 equivalent maxima at the C_3 points, 6 equivalent minima at the C_4 points, and 12 saddle points at the C_2 points. We shall use this as an example in the following to state the form of an approximate quantization condition and to illustrate the correlation to the pattern of clusters.

Let us call the energy of the eight maxima E_{max}, that of the six minima E_{min}, and that of the saddle points E_{sad}. If we choose an energy value E_{cl} between E_{min} and E_{sad}, we may illustrate this by a perfect sphere of radius E_{cl}. This sphere will intersect the rotational energy surface along six closed contour curves which are more or less deformed circles with centers on the C_4 axes. This 6-fold degeneracy is what causes the formation of a 6-fold cluster. The six contour curves are identical in shape, and they each enclose an approximately plane figure. The area A of this figure may be used to express the quantization condition, simply by requiring this area to be proportional to the cluster index τ plus one half,

$$A \propto \tau + \frac{1}{2}. \tag{4}$$

Unfortunately, it is complicated to express the proportionality constant explicitly. It is, however, not needed for the purpose of the present paper where we use mainly qualitative arguments. More rigorous formulations may be found in the literature, for instance in Ref. (*17*).

The quantization condition expressed by Eq. (4) is closely analogous to that of the linear harmonic oscillator, and it yields a number of equidistant energy values starting by half a step. In the present case, it means that the quantization condition is satisfied for a number of equidistant values of E_{cl} starting half a step above E_{min}. At each of these energies a 6-fold cluster will appear, characterized by a cluster index $\tau = 0, 1, 2, \ldots$ starting with $\tau = 0$ for the cluster with energy E_{cl} closest to E_{min}. It should be emphasized, however, that this simple form of the quantization condition is only approximate, but becomes better the closer E_{cl} is to E_{min}, mainly because it assumes that the rotational energy may be approximated by a second-order surface in the neighborhood of a minimum. As E_{cl} comes close to E_{sad}, the contour curves come

closer to one another, and it becomes very complicated to express the quantization condition. In the quantum mechanical description and in the experiment, this manifests itself by a broadening of the clusters with increasing values of the cluster index τ, and it finally becomes a matter of definition whether a cluster is present or not. The present quantization condition seems sufficient for qualitative or semiquantitative comparisons between the model on the one side and the experiment or calculations based on quantum mechanics on the other.

If, instead, we chose the energy E_{cl} to be between E_{sad} and E_{max}, the constant energy sphere will intersect the rotational energy surface along eight closed contour curves near the C_3 points. The quantization condition is the same as above, and the result is a series of almost equidistant 8-fold clusters where the cluster with index $\tau = 0$ is closest to E_{max}. Again the series deteriorates when E_{cl} comes close to E_{sad}. In both series the clusters will only be equidistant as long as the rotational energy surface is a second-order surface with good accuracy, which will be the case for sufficiently low values of the cluster index τ. In the following, each cluster will for convenience be indicated by the degeneracy with the cluster index as a subscript; e.g., 6_0 for the first cluster in the series of 6-fold clusters.

The approximate quantization condition discussed here is by far the most important. There are, however, special cases where certain parts of the rotational energy surface have sufficiently simple forms so that it is possible to derive other approximate quantization conditions. One such example is discussed below in connection with folded series of clusters. The details of the derivation in this special case is given in the Appendix.

PATTERN OF CLUSTERS IN ONE MANIFOLD

Type I

The most commonly observed pattern of clusters for any manifold of rotation–vibration states in any of the three isotopic species of CF_4 is the one described above, corresponding to the shape of the rotational energy surface indicated as No. 1 in Table I. It is characterized by two series of clusters, one series of 6-fold clusters starting with $\tau = 0$ at the low energy end of the manifold and another series of 8-fold clusters starting with $\tau = 0$ at the high energy end of the manifold. Where these two series meet, close to E_{sad}, a number of states do not appear in clusters but rather form a kind of transition region from one series to the other. This is the pattern of clusters termed type I in Ref. (*3*).

In Fig. 2 of Ref. (*3*) an energy level diagram is given for the $J = 60$ manifold of the vibrational ground state of $^{12}CF_4$. It is seen that the clusters are indeed approximately equidistant, but the deviation from this is significant, even for low values of τ, in agreement with the fact that the rotational energy surface can never be precisely a second-order surface.

The length of the two series varies over a wide range for different manifolds. For the vibrational ground state the 6-fold series is generally three times as long as the 8-fold series. In the semiclassical model this means that the six minima at the C_4 points on the rotational energy surface are much more prominent than the eight maxima at the C_3 points when measured from the level of the saddle points; in other words $E_{sad} - E_{min} \approx 3(E_{max} - E_{sad})$. In other vibrational components, the proportion between the length of the two series is often very different from the case of the vibrational ground state. One of the two series may thus contain only one cluster (with $\tau = 0$)

or it may be missing completely. This corresponds to the case where either the maxima or the minima are so flat that the quantization condition will only be satisfied for one value of E_{cl} or, because of the $\frac{1}{2}$, not at all.

Type II

Also very common is the pattern of clusters termed type II in Ref. (*3*). This corresponds to the shape of the rotational energy surface indicated as No. 2 in Table I. It is simply the reversed situation of type I in the sense that the series of 6-fold clusters appear with the 6_0 cluster at the high-energy end of the manifold, whereas the series of 8-fold clusters appear with the 8_0 cluster at the low-energy end of the manifold. Otherwise the pattern of clusters and the transition region are analogous to the type I case.

If one calculates the energies within a certain manifold by means of an effective Hamiltonian truncated after the centrifugal distortion term $cR^{4(4,A_1)}$ the resulting pattern of clusters will be either of type I or of type II depending on the sign of the coefficient c (*18, 19, 12*). Also, one obtains a precise value of 3 for the proportion of the length of the 6-fold series to that of the 8-fold series.

Three Series of Clusters (12-Fold Clusters)

While the first two shapes given in Table I indicate one type of maxima and one type of minima on the rotational energy surface, leading to two well-separated series of 6-fold and 8-fold clusters, each of the following six shapes in Table I indicates three types of maxima or minima, leading to three series of clusters, one 6-fold, one 8-fold, and one 12-fold. In these cases two of these series must proceed more or less from one end of the manifold and the third series from the other end.

As an example, Fig. 2 gives the energy level diagram of the $J = 45$ manifold of the $D_g^{(J)}$ vibrational component of the $3\nu_2(A_1 + A_2)$ vibrational state of $^{12}CF_4$, showing three series of clusters. The series of 12-fold clusters starts at the top of the manifold, and the two other series start almost at the same energy at the bottom of the manifold. This example corresponds to shape No. 4 in Table I. From the energy interval covered by each series it is seen that the maxima at the 12 C_2 points on the rotational energy surface are rather prominent compared to the 24 σ_{34} saddle points, whereas the minima at the 6 C_4 points and the minima at the 8 C_3 points are less prominent and of about the same depth.

Compared to the ground state manifold discussed above, the series in this manifold are much shorter. The high degeneracy of the 12-fold clusters leaves no possibility for long series, except for very high values of J. The example chosen here is in fact an exception with respect to the length of the 12-fold series. Usually it consists of one or two clusters only. If the energy corresponding to the maxima or minima at the 12 C_2 points is very close to the energy of the saddle points, the 12-fold series may not show up at all, and the pattern of clusters is effectively reduced to type I or II. Similarly the 6-fold or the 8-fold series may be missing if the corresponding maxima or minima are very flat.

In order to compute manifolds including 12-fold clusters from effective Hamiltonians one also has to include in this the $R^{6(6,A_1)}$ term (*20*).

24-Fold Clusters

So far we have discussed only the first eight shapes of the rotational energy surface indicated in Table I. All other shapes will include at least one set of maxima or minima

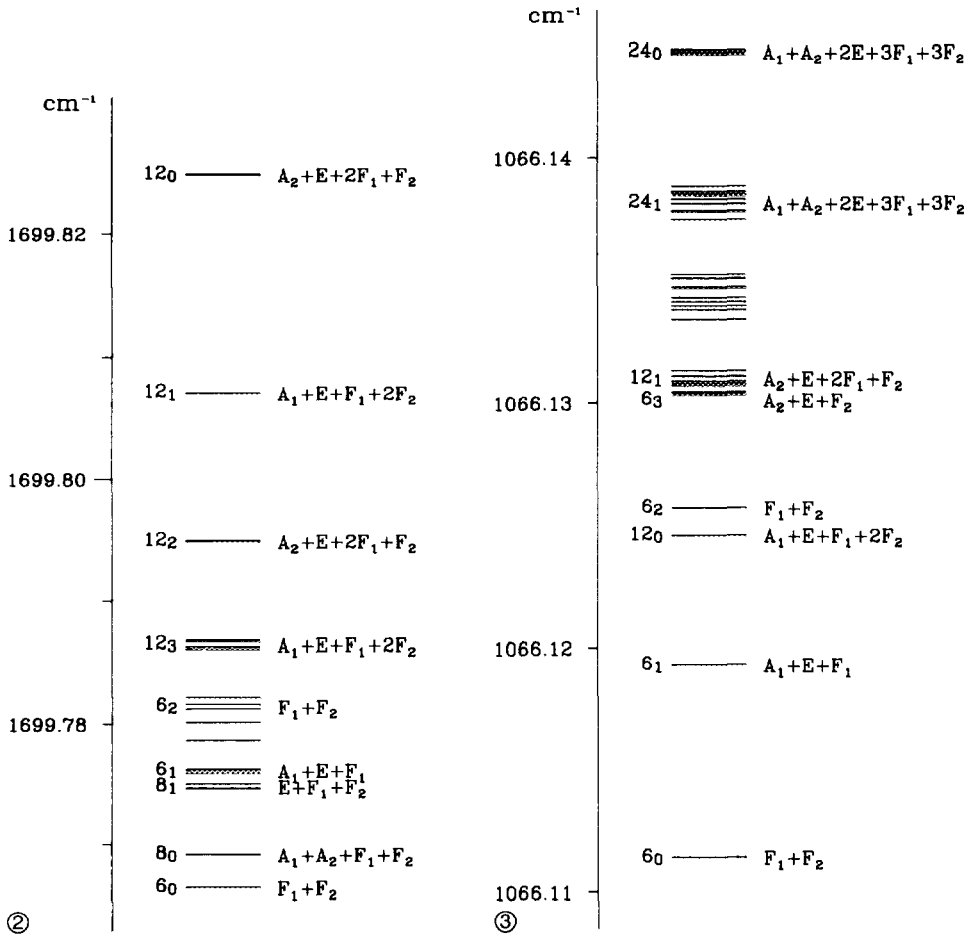

FIG. 2. The energy level diagram for the $J = 45$ manifold of the $D_g^{(J)}$ vibrational component of the $3\nu_2(A_1 + A_2)$ vibrational state of $^{12}CF_4$ showing one series of 6-fold clusters, one of 8-fold clusters, and one of 12-fold clusters. Each cluster is indicated by the degeneracy with the cluster index as a subscript and by the rotation–vibrational symmetry of the states forming the cluster.

FIG. 3. The energy level diagram for the $J = 57$ manifold of the $D_u^{(J+2)}$ vibrational component of the ν_2 vibrational state of $^{12}CF_4$ showing the presence of 24-fold clusters.

outside the C_4, C_3, or C_2 points, usually at some σ point as a set of 24 maxima or minima. If these maxima or minima are prominent enough, they will lead to the formation of a series of 24-fold clusters.

Twenty-four-fold clusters are very rare. We have found them only in the $D_u^{(J+2)}$ vibrational component of the ν_2 and the $\nu_1 + \nu_2$ vibrational states of all three isotopic species for J values close to 57. In this case there are minima at all C_4, C_3, and C_2 points, saddle points at a set of σ_{24} points, another set of saddle points at a set of σ_{23} points, and maxima only at a set of σ_{34} points (see shape No. 27 in Table I and Fig. 9c). It is these maxima which give rise to the 24-fold clusters appearing at the maximum energy end of the manifold.

Figure 3 gives the energy level diagram of the $J = 57$ manifold of the $D_u^{(J+2)}$ vibra-

tional component of the ν_2 vibrational state of $^{12}CF_4$. The cluster indices for the 6-fold, 8-fold, and 12-fold clusters have been determined in the usual way from the k-distributions of the computed wavefunctions (*3*). A similar determination for the 24-fold clusters is difficult because the precise position of the σ_{34} maxima is not determined by symmetry, and the angles by which the wavefunctions should be rotated (*3*) are thus unknown. The cluster indices indicated in the figure are derived simply from the position of each cluster. From Table IV of Ref. (*3*) it is immediately obvious that any 24-fold cluster must have the symmetry $A_1 + A_2 + 2E + 3F_1 + 3F_2$ equal to the total symmetry of a complete cycle of four 6-fold clusters or three 8-fold clusters. The symmetry is thus independent of the cluster index, which means that the symmetry unfortunately cannot be used to check the assignment of τ.

Twenty-four-fold clusters have never been discussed before within molecular spectroscopy or dynamics, but only in more general theories (*16*). In principle, a set of 48 maxima or minima at one of the general points C_1 might lead to the formation of 48-fold clusters. We have seen no indication of the presence of such clusters.

Folded Series of Clusters

There are at least two reasons why 24-fold clusters are so rare. First, the total degeneracy of the manifold must be high to give room for 24-fold clusters in addition to two (or three) series of more ordinary clusters. This means that 24-fold clusters can only appear at high J values. Second, there is in practice a marked tendency for the presence of maxima or minima at the σ points not to lead to a series of 24-fold clusters but to the formation of a folded series of 6-fold or 8-fold clusters. We shall discuss this phenomenon by means of the $J = 45$ manifold of the $D_g^{(J+1)}$ vibrational components of the $\nu_2 + \nu_4$ vibrational state of $^{12}CF_4$. The energy level diagram of this manifold is shown in Fig. 4. The determination of the cluster indices for the folded series of 6-fold clusters in this manifold from the k-distributions of the wavefunctions has been discussed in detail in Ref. (*3*). Here we shall give the explanation of the folding in terms of the shape of the rotational energy surface.

In order to see what the shape of the surface is in this case it is useful to consider it as a development from the shape corresponding to the type II pattern of clusters, given as No. 2 in Table I. In that case there is a maximum at any C_4 point. We may now introduce the qualitative change of the surface indicated in the second line of Table II, resulting in a change of each of the maxima at the C_4 points into a local minimum surrounded by four maxima at σ_{24} points and four saddle points at σ_{34} points. If these four maxima and four saddle points are moved a little away from the C_4 point, the resulting surface is as illustrated by Fig. 5. In the actual case the difference in energy between the new maxima and saddle points is so small that the $\frac{1}{2}$ in the quantization condition prevents the formation of 24-fold clusters due to the 24 maxima at the σ_{24} points. Instead, the four maxima and the four saddle points form an almost circular ridge around the minimum. This results in the formation of a series of 6-fold clusters, for which the deformed circle starts near the minimum at the C_4 point, goes first up to the almost circular ridge, and then proceeds toward lower energies as usual. The energies of the clusters as a function of the cluster index τ consequently go through a maximum.

Clearly, the usual quantization condition cannot be applied when the deformed circles are close to the circular ridge. Instead, another approximate condition may be developed, as shown in the Appendix. The result is that the energy of the clusters as a function of the cluster index τ, after the usual approximately straight line for low

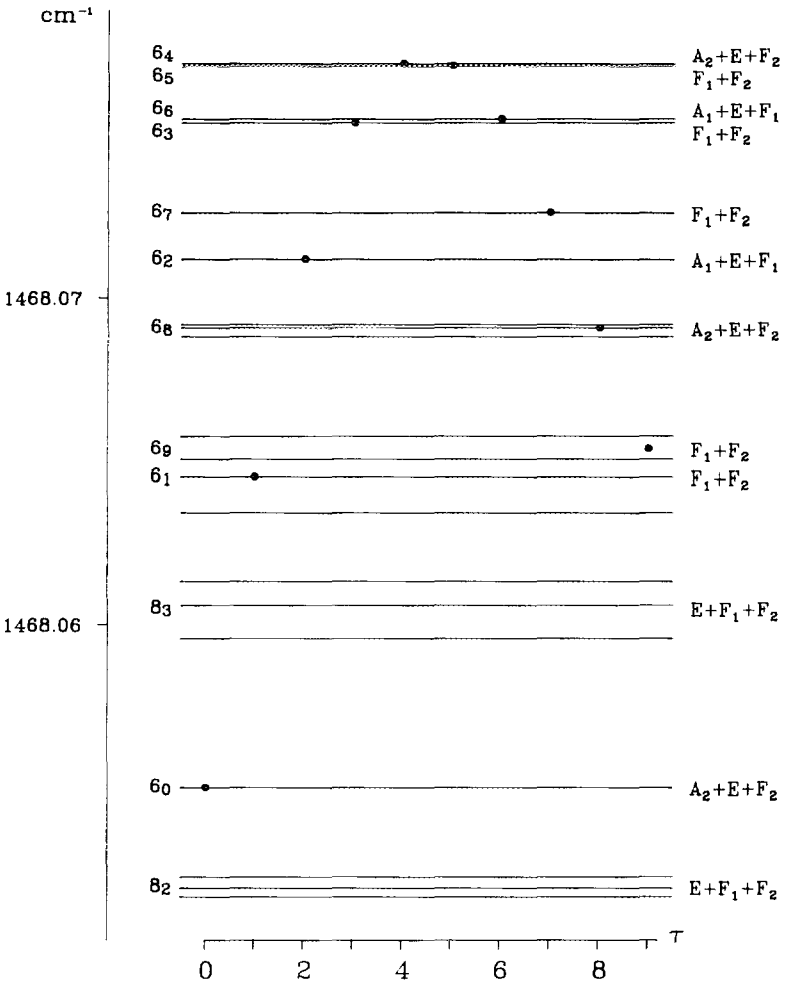

FIG. 4. The energy level diagram for the $J = 45$ manifold of the $D_g^{(J+1)}$ vibrational components of the $\nu_2 + \nu_4$ vibrational state of $^{12}CF_4$ showing a folded series of 6-fold clusters. The energy of the clusters as a function of the cluster index τ is shown by means of a dot for each cluster.

values of τ, should follow a parabola, corresponding to a position of the deformed circles near the circular ridge, and possibly end in another approximately straight line when the deformed circles have passed the circular ridge. A plot of the energy of the folded series of 6-fold clusters versus τ is included in Fig. 4 by means of a τ axis and a dot for each cluster. The energies are seen to follow the expected curve very nicely.

Folded series of clusters appear quite often and in different versions. It is immediately clear that if all maxima in the present example are replaced by minima and all minima by maxima, the circular ridge is replaced by a circular depression around a maximum at the C_4 point, and the result is a folded series of 6-fold clusters with the bend at the low-energy end of the manifold. But it is also possible to find folded series of 8-fold clusters. These are due to a formation of an almost circular ridge or depression around each of the C_3 points, caused for instance by a set of σ_{34} maxima and a set of σ_{23} saddle points.

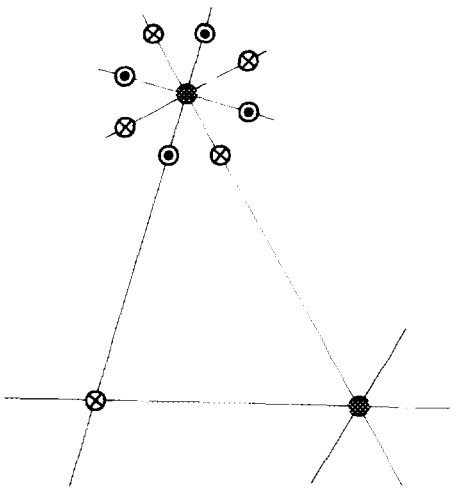

FIG. 5. The shape of the rotational energy surface responsible for the formation of the folded series of 6-fold clusters shown in Fig. 4, indicated by means of a diagram of one of the 48 spherical triangles, analogous to the one shown in Fig. 1. Maxima are indicated by ⊙, minima by ●, and saddle points by ⊗.

If the rotational surface has, for instance, one set of maxima at some σ_{34} and two sets of saddle points, one at a σ_{24} point and the other at a σ_{23} point, it is clear from the above discussion that three different patterns may result: (i) a folded 6-fold series, folding at the high-energy end of the manifold; (ii) a series of 24-fold clusters starting at the high-energy end of the manifold; or (iii) a folded 8-fold series, folding again at the high-energy end of the manifold. In the discussion given below of the pattern of the $D_u^{(J+2)}$ vibrational component of the ν_2 vibrational state as a function of J, we show how the variation of the pattern with J is explained partly as a continuous transformation from the first of these possibilities over the second one to the third one, due to a quantitative change of the surface, resulting primarily in a displacement of a set of σ_{34} maxima from a position near the C_4 point, through a position near the midpoint between the C_4 and the C_3 points, to a position near the C_3 point. From this example it is tempting to conclude that the choice between the three possibilities in general depends on the precise position of the maxima (or minima) at the σ_{34} points, but this is only an idea open to future discussion.

In order to compute manifolds with folded series of clusters from effective Hamiltonians, one has to include also the $R^{8(8,A_1)}$ term (*21*).

THE PATTERN OF CLUSTERS WITHIN ONE ISOLATED VIBRATIONAL COMPONENT AS A FUNCTION OF J

The type I pattern of clusters is the most commonly observed in the 6500 or so computed manifolds. For $^{12}CF_4$ there are 9 vibrational components in which all manifolds for $J \leqslant 70$ are of type I (*3*). For the two other isotopic species the situation is similar. Also, the type II pattern of clusters is observed quite often, but in $^{12}CF_4$ only one vibrational component is exclusively of type II.

In many other vibrational components, type I manifolds appear for J below a certain limit, and often only type II manifolds are present above a higher value of J. The manifolds for J between these two limits represent an almost continuous trans-

formation, resulting in an inversion of the type I pattern into the type II pattern. Or the situation may be the reversed one with type II manifolds up to a certain value of J, a region of inversion, and type I manifolds for J above some higher value. The present section is devoted to a rather detailed description, based on Table II, of how this inversion may take place, so to speak, as a function of J. Only isolated vibrational components are treated in this paper. Overlapping components and intersecting components represent different problems which will be treated elsewhere (*22*).

We shall relate the changes in the patterns of clusters during an inversion to the corresponding changes in the shape of the rotational surface. One might imagine that the simplest way for these changes to take place would be that the rotational energy surface be transformed directly through a perfect sphere to the new form. But this is never the case because of the restrictions placed on qualitative changes in the shape of the rotational surface, as indicated by Table II. Instead, the transformation takes place through a number of intermediate shapes of the surface, where the formation of new saddle points causes consecutive transformations of maxima into minima and vice versa. The details of these transformations may differ significantly, but it is possible to sort out two main types, the simple inversion and the complex inversion. In the following these two types will be discussed in detail, partly by means of two examples.

The Simple Inversion

In order that an inversion may take place, the maxima (or minima) at the C_4 points must be changed into minima (or maxima), and the minima (or maxima) at the C_3 points must be changed into maxima (or minima) as a consequence of a change in J. From the above discussion of the possible qualitative changes of the rotational surface, it is clear that such a change at the C_3 points can only take place as the consequence of a passage of saddle points. The simplest way to obtain the corresponding change at the C_4 points is then to let the same saddle points also pass the C_4 points. The simplest way to create these saddle points is to let the C_2 saddle points change into maxima or minima with a simultaneous creation of σ_{23} or σ_{24} saddle points. These may then move around the spherical triangles, passing both the C_3 and the C_4 points, and finally change the C_2 points back into saddle points as they disappear. These are the changes of the shape of the surface corresponding to any simple inversion (*9, 23*). It should be emphasized, however, that the primary event is a change of the molecular geometry due to a change of J, and this change of the molecular geometry gives rise to a change of the rotational surface, the essence of which may be described as this moving of the saddle points.

The simple inversion is thus initialized by a creation of the σ saddle points, but this is not observed directly in the pattern of clusters. What is seen is the appearance of a series of 12-fold clusters due to the formation of maxima (or minima) at the C_2 points. Then either the C_4 points or the C_3 points are changed from maxima to minima or vice versa. This is observed first as a disappearance of the 6-fold or the 8-fold series, followed by a reappearance of the same type of series starting from the other end of the manifold. Next the other series is transformed in an analogous way, and finally the 12-fold series disappears as the σ saddle points turn the C_2 points back into saddle points.

As an example of the simple inversion we discuss in detail the inversion in the $D_g^{(J+2)}$ vibrational component of the $2\nu_4$ vibrational state of $^{12}CF_4$. This component is well isolated and shows the type II pattern of clusters for $J \leqslant 31$ and type I for $J \geqslant$

38. The inversion thus takes place over the eight values of J from 31 to 38. Figure 6 gives the energy level diagrams for $30 \leqslant J \leqslant 39$, all on the same scale, but displaced as indicated. The corresponding changes in the shape of the rotational energy surface are sketched in Fig. 7 by means of a number of drawings, each of which is analogous to Fig. 5. The following discussion thus refers to Figs. 6 and 7 simultaneously, and also to Table II.

The manifolds for $J \leqslant 31$ are all of type II, but the 8-fold series is extremely short, consisting of the 8_0 cluster only, and even this disappears at $J = 31$, whereas the 6-fold series is very long. This means that the maxima at the C_4 points are prominent, whereas the energy of the minima at the C_3 points is close to that of the C_2 saddle

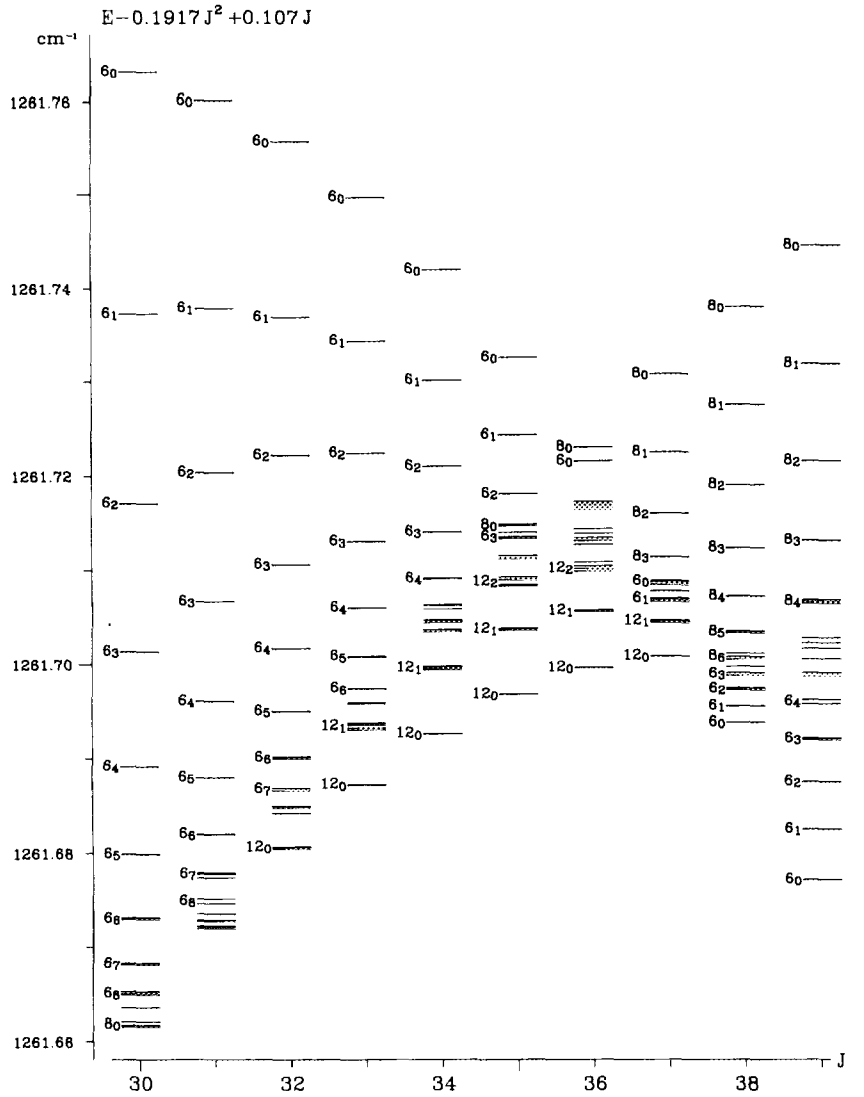

FIG. 6. The reduced energy level diagrams for the $D_g^{(J+2)}$ vibrational component of the $2\nu_4$ vibrational state of $^{12}CF_4$ for $30 \leqslant J \leqslant 39$ demonstrating the details of a simple inversion. The energy has been reduced as indicated to fit all diagrams on the same figure.

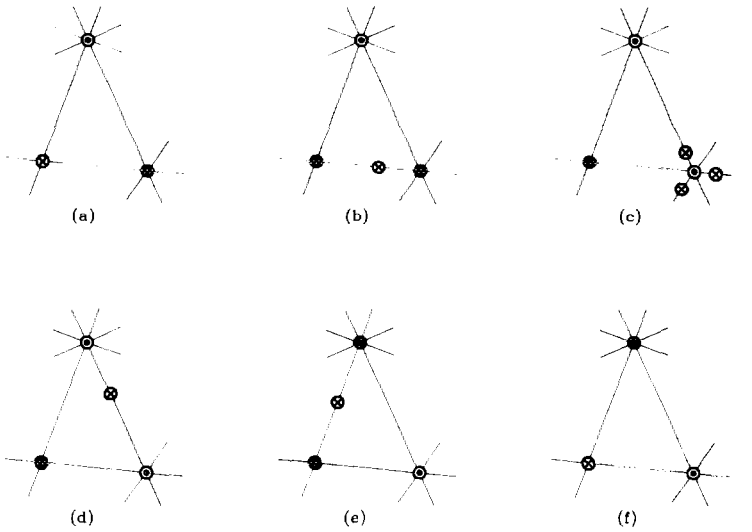

FIG. 7. The changes in the shape of the rotational energy surface responsible for the simple inversion shown in Fig. 6, illustrated by six drawings, each of which is analogous to Fig. 5. Maxima are indicated by ⊙, minima by ●, and saddle points by ⊗.

points (see Fig. 7a). In other words, the surface is close to a sphere, except for the six prominent maxima at the C_4 points.

As stated above, the start of the inversion is observed in the energy level diagram by the appearance of a series of 12-fold clusters starting at the low-energy end of the manifold. This is due to the formation of minima at the C_2 points, simultaneously with the formation of a set of σ_{23} saddle points, as given by line No. 7 in Table II, if maxima are replaced by minima. The resulting shape of the rotational energy surface is indicated in Fig. 7b. The series of 12-fold clusters is seen for all J values from 32 to 37. For $J = 32$, 33, and 34 the manifold thus contains two series of clusters, a short 12-fold series at the low-energy end and a long 6-fold series at the high-energy end. There is no 8-fold series; it is prevented from appearing by the surface being too close to a perfect sphere near the C_3 points.

The passage of the σ_{23} saddle points through the C_3 points and the change of the minima at the C_3 points into maxima corresponds to line No. 4 in Table II if maxima are replaced by minima and minima by maxima. The resulting shape of the surface is sketched in Fig. 7c. This change of the surface does not show up in the pattern of clusters because the surface is still very flat around the C_3 points until the new σ_{34} saddle points are far from the C_3 points, allowing the maxima at the C_3 points to be prominent enough that a new series of 8-fold clusters is formed for $J \geqslant 35$. In principle, there is now both a 6-fold and an 8-fold series starting from high energies. For $J = 35$ the 8-fold series only shows up as an 8_0 cluster, appearing in the middle of the manifold. For $J = 36$ the 8_0 is at the high-energy end of the manifold, with the 6-fold series starting at a slightly lower energy, but now only consisting of the one 6_0 cluster. This means that most of the surface is very close to a perfect sphere. The maxima at the C_3 points are now the most prominent ones, and a large part of the inversion has been carried through. At $J = 37$ the 8-fold series has increased to four members. This shows that the σ_{34} saddle points are now rather close to the C_4 points (Fig. 7d).

Next the σ_{34} saddle points pass the C_4 points, transforming them into minima, as given by line No. 3 in Table II. The shape of the resulting surface is outlined in Fig. 7e, but the corresponding pattern is not seen in the energy level diagrams; it is, so to speak, hidden between $J = 37$ and $J = 38$. The inversion is completed by the σ_{24} saddle points transforming the C_2 points into saddle points, as given by line No. 8 in Table II when read from right to left and replacing maxima with minima. The resulting shape of the surface, outlined in Fig. 7f, is the one which corresponds to the type I pattern of the clusters, and this is precisely what is seen in the energy level diagrams for $J \geqslant 38$ showing a long 8-fold series from the high-energy end of the manifold and a somewhat shorter 6-fold series from the low-energy end of the manifold.

The simple inversion has been seen in six different vibrational components of $^{12}CF_4$, but the inversion is only complete in two components; in the other four cases the component mixes with some other component before the inversion is complete.

There is by no means a linear relation between the J value and the single steps in the changes in the pattern of clusters due to the different changes of the shape of the surface. This is caused by the nonlinear relation between changes in J and the changes in the moments of inertia and in the potential energy. This nonlinearity is nicely demonstrated by the example used above, showing how one change in the shape of the surface may correspond to several J values, whereas some other steps do not show up at all because they are performed between neighboring J values. It is this complicated behavior of the pattern of clusters which makes the assignment of inversions a nontrivial problem.

The Complex Inversion

The complex inversion differs from the simple one in that the inversion at the C_4 points is not caused by a passage of some saddle points, but by the simultaneous creation both of a set of σ minima (or maxima) and of a set of σ saddle points, giving rise either to a folded series of 6-fold clusters or to the formation of 24-fold clusters, as discussed above. The inversion at the C_3 points must be caused by a passage of saddle points, as follows from Table II. These saddle points may either be the ones just mentioned, originating at the C_4 points, or they may, as in the simple inversion, be created at the C_2 points, giving rise also to the creation of a series of 12-fold clusters. However, we have seen no sign of the first possibility, so we do not discuss it further. After the passage of the C_3 points the σ_{34} saddle points originating at the C_2 points and the σ_{34} maxima (or minima) from the C_4 points annihilate each other, as indicated by line No. 11 of Table II. The σ_{24} saddle points created at the C_4 positions move to the C_2 points and turn these back into saddle points, as in the simple inversion, causing the series of 12-fold clusters to disappear at the end of the complex inversion. There is a large number of possibilities for the details of complex inversions, but those observed are all of the type discussed below.

We exemplify the complex inversion by the $D_u^{(J+2)}$ vibrational component of the ν_2 vibrational state of $^{12}CF_4$. All manifolds are of type II for $J \leqslant 48$ and of type I for $J \geqslant 63$, and the inversion thus takes place in the interval from $J = 49$ to 62. Figure 8 indicates the energy level diagrams for $47 \leqslant J \leqslant 60$, all on the same scale, but displaced as indicated. The corresponding changes in the shape of the rotational energy surface are outlined in Fig. 9 by means of a number of drawings analogous to Fig. 7.

For $J \leqslant 48$ the cluster pattern is of type I, although the two first clusters in the 6-fold series are rather close at $J = 48$. The corresponding shape of the rotational energy

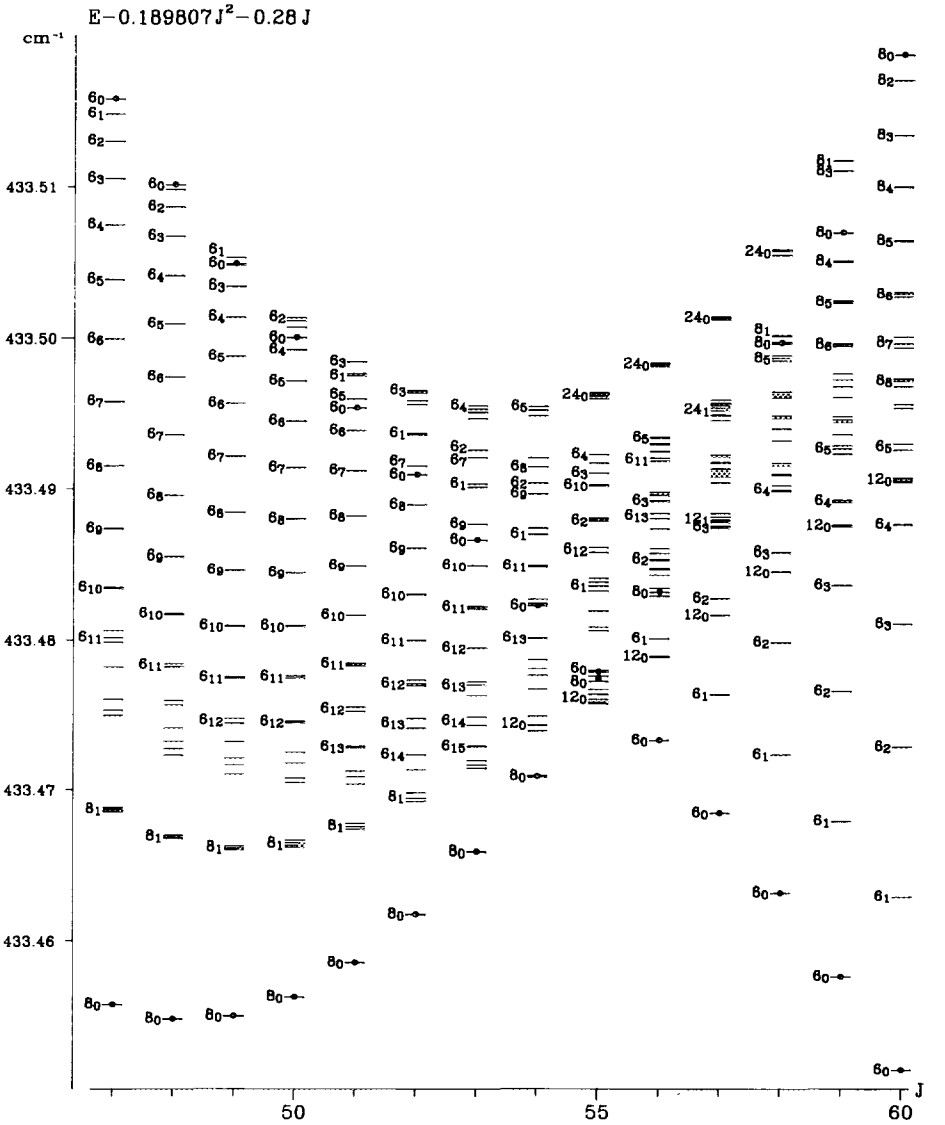

FIG. 8. The reduced energy level diagrams for the $D_u^{(J+2)}$ vibrational component of the ν_2 vibrational state of $^{12}CF_4$ for $47 \leq J \leq 60$ demonstrating the details of a complex inversion. In the regions where the clusters are very close some cluster symbols have been left out. The 6_0 and 8_0 clusters are marked by dots. The energy has been reduced as indicated to fit all diagrams on the same figure.

surface is thus the simple one indicated in Fig. 9a. At $J = 49$ the 6-fold series starts to fold at the high-energy end of the manifold. As discussed above this folding is caused by a change of the maxima at the C_4 points to minima and a simultaneous creation of 24 σ_{24} saddle points and 24 σ_{34} maxima, as indicated by line No. 1 in Table II. The resulting shape of the surface is shown in Fig. 9b.

The bending of the 6-fold series increases with J, so that at $J = 53$ the 6_4 cluster has the highest energy within the manifold. This is the result of a deepening of the C_4

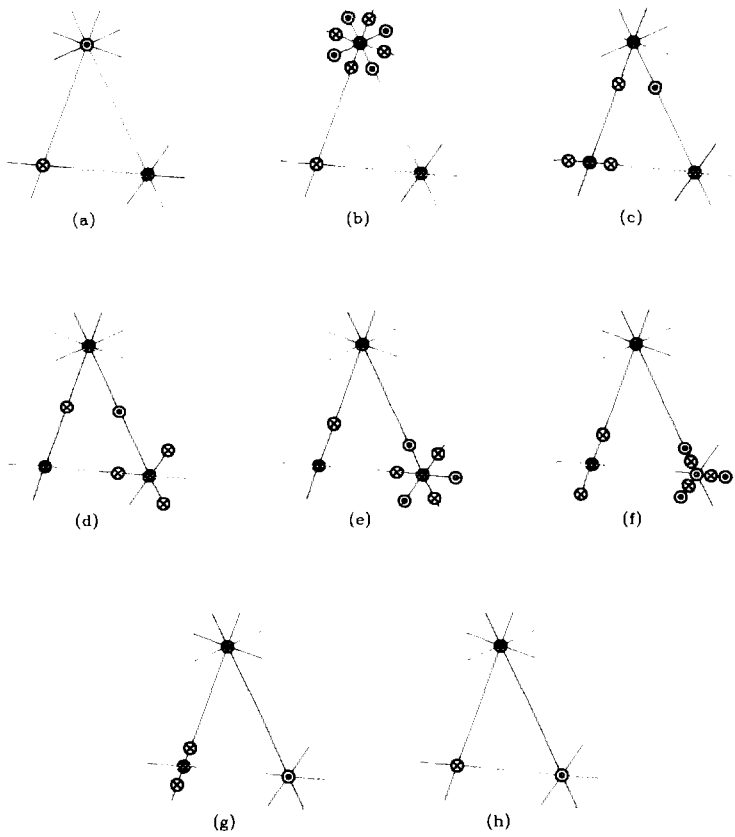

FIG. 9. The changes in the shape of the rotational energy surface responsible for the complex inversion shown in Fig. 8, illustrated by eight drawings, each of which is analogous to Fig. 5. Maxima are indicated by ⊙, minima by ●, and saddle points by ⊗.

minima and a simultaneous moving away from the C_4 points of the σ_{24} saddle points and the σ_{34} maxima, as indicated by Fig. 9c.

At about $J = 53$ the C_2 saddle points are transformed into minima, simultaneously with the formation of 24 new σ_{23} saddle points, also indicated in Fig. 9c. The result is the appearance from $J = 54$ to $J = 62$ of a series of 12-fold clusters, usually consisting of only the 12_0 cluster, but for $J = 57$, also of a 12_1 cluster, the position of which demonstrates that minima, not maxima, have been created at the C_2 points by the process indicated in line No. 7 in Table II if maxima are replaced by minima.

Already at $J = 53$ it is possible to postulate the presence of one 24_0 cluster instead of the four 6-fold clusters of highest energy. As J increases such a conversion of 6-fold clusters into 24-fold clusters becomes more and more obvious, until at $J = 57$ the eight 6-fold clusters of highest energy have disappeared completely, being replaced by the 24_0 and 24_1 clusters, as discussed above. Probably the corresponding shape of the surface is close to the one indicated by Fig. 9d. As J increases further, the 24-fold clusters are gradually transformed into a folded series of 8-fold clusters, as clearly seen at $J = 59$. This series is the same as the one observed as a very short series for $J \leqslant 56$. It has disappeared completely at $J = 57$ because the surface is too flat round the C_3 points, but for $J = 58$ and 59 the minimum is apparently more prominent. The

folding of the 8-fold series is caused by the σ_{34} maxima, created at the C_4 points, and the σ_{23} saddle points, created at the C_2 points, forming an almost circular ridge around the C_3 points, as shown in Fig. 9e. Note that the shapes given by Figs. 9c, 9d, and 9e differ only quantitatively, as discussed above.

Between $J = 59$ and $J = 60$ the σ_{23} saddle points pass through the C_3 points, in agreement with line No. 4 of Table II if maxima are replaced by minima and minima by maxima. The resulting shape of the surface for $J = 60$ may be the one indicated in Fig. 9f or the 24 σ_{34} maxima and the 24 σ_{34} saddle points may already have cancelled each other, leaving just a slope from the minima at the C_4 points to the maxima at the C_3 points, as indicated by line No. 11 of Table II if read from right to left. In the last case the shape of the surface is given by Fig. 9g. For $J = 60$ the energy of the 8_1 cluster is only slightly less than that of the 8_0 cluster (they cannot be distinguished in Fig. 8), showing that the maxima at the C_3 points are rather deformed, but for $J \geq 61$ the series of 8-fold clusters is a normal and rather prominent series, indicating that the maxima at the C_3 points are now of the usual shape and of rapidly increasing prominence as J increases.

The complex inversion is completed by the 24 σ_{24} saddle points moving into the C_2 points, transforming the minima into saddle points, as given by line No. 8 of Table II if read from right to left and if maxima are replaced by minima. This causes the series of 12-fold clusters to disappear from $J \approx 62$. The final shape of the surface is thus the simple one given in Fig. 9h for $J \geq 63$.

In Fig. 8 all the 6_0 and 8_0 clusters have been marked by a dot to make it easier to follow how these limiting clusters interchange their positions very smoothly as a function of J.

This example of the complex inversion is very nearly duplicated not only in the $D_u^{(J+2)}$ vibrational components of the ν_2 vibrational state of $^{13}CF_4$ and $^{14}CF_4$, but also in the $D_u^{(J+2)}$ vibrational component of the $\nu_1 + \nu_2$ vibrational state of all three isotopic species. The complex inversion is seen also in other vibrational components, but no 24-fold clusters are formed, in most cases probably just because the J value is too low to give room for clusters of such a high degeneracy. Inversions are seen both, as here, from type II to type I and from type I to type II. In the model this only corresponds to an interchange of maxima and minima. For $^{12}CF_4$ a total of six complex inversions are seen, out of which the five are complete inversions, whereas the sixth is incomplete because of a crossing with some other vibrational component.

Width of the Manifolds

In connection with the inversion it is interesting to look at the width of the manifolds within one isolated vibrational component as a function of J. By the width of a single manifold we understand the difference between the highest and the lowest energy in that manifold. Apart from two half-quanta the width equals $E_{max} - E_{min}$, as defined above, and is thus a reasonable measure of the deviation of the rotational energy surface from a perfect sphere. This deviation is due to centrifugal distortion of the equilibrium geometry of the molecule, depending in a complicated way on the deformation of the molecule due to vibrational movements.

Figure 10 shows a plot of the widths of the manifolds within three different vibrational components as a function of J. The simplest case is that of the vibrational ground state. Here the rotational energy surface has shape No. 1 (see Table I) throughout,

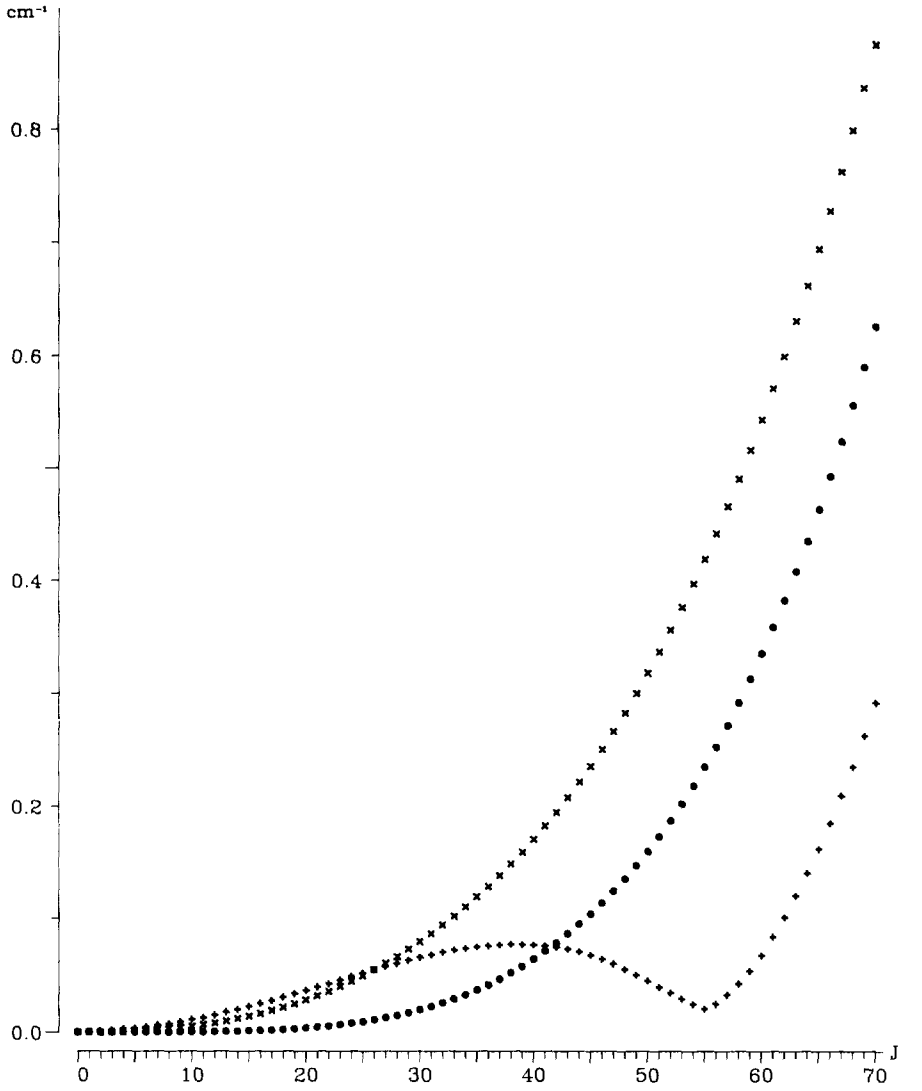

FIG. 10. The width of the manifolds of the vibrational ground state (●), the $D_g^{(J-2)}$ vibrational component (×), and the $D_u^{(J+2)}$ vibrational component (+), both of the ν_2 vibrational state. The last case illustrates the effect of an inversion.

and the width increases regularly as a function of J, because the centrifugal distortion of the geometry naturally increases when the molecule rotates faster.

The next case is that of the $D_g^{(J-2)}$ vibrational component of the ν_2 vibrational state of $^{12}CF_4$. Again the width increases regularly as a function of J, but more rapidly than that for the vibrational ground state. This indicates that the effect of the vibrational movements in this component of ν_2 adds to the rotational effect, increasing the centrifugal distortion compared to the vibrational ground state.

The third case is that of the $D_u^{(J+2)}$ vibrational component of the ν_2 vibrational state of $^{12}CF_4$, showing the effect of the complex inversion. Here the vibrational effect counteracts the rotational effects for J larger than about 25, causing the width to go

through a very deep minimum at $J = 55$ which is in the middle of the region of the inversion. This minimum is also clearly seen in Fig. 8. In fact the width for $J = 55$ is only 5% of the width of the other vibrational component of ν_2. In terms of the shape of the rotational surface, this means that the surface deviates most from the ideal sphere when the shape is No. 1 (see Table I) as for $J \leqslant 48$ or No. 2 as for $J \geqslant 63$, whereas the surface is closer to the ideal sphere for the shapes of higher numbers. The inversion goes through shapes very close to the ideal sphere, but the interesting point is that these shapes have a higher number of maxima and minima than shape Nos. 1 and 2. In other words, shape Nos. 1 and 2, with few maxima and minima, represent two opposite extremes of a highly deformed rotational surface, and the transformation from one to the other goes through shapes with more maxima and minima, smoothing out the surface, not through the extremely improbable case of the ideal sphere, but through the formation of a large number of small maxima and minima. Physically this is the most probable way, although mathematically it looks quite complicated.

QUANTITATIVE APPLICATIONS TO THE VIBRATIONAL GROUND STATE

The main virtue of the semiclassical model is its ability to yield qualitative information on the possible degeneracies of the clusters, on the different patterns of clusters, on the possible changes of these patterns, etc. Generally it is not recommended to use it quantitatively, for instance to make predictions of the patterns of clusters. Such calculations are better performed by means of precise quantum mechanical calculations based on a diagonalization of the Hamiltonian matrix. We have, however, found it interesting to make a calculation of the energy values E_{max}, E_{min}, or E_{sad} in the simple case of the vibrational ground state, in order to see how well it is possible to reproduce by means of the semiclassical model the much more accurate values from the quantum mechanical model.

These calculations are based on the following principles which may be considered as extensions of the semiclassical model. The classical energy of the molecule is a sum of the rotational energy, the vibrational energy, and the potential energy. For the vibrational ground state the vibrational energy is set equal to zero. The rotational energy is replaced by

$$E_{rot} = \frac{\hbar^2 J^2}{2I}, \tag{5}$$

where I is the moment of inertia around the actual axis of rotation. Instead of J^2 one might use $J(J + 1)$, but it does not make any great difference to the final results. For the potential energy we use the harmonic part of the potential function (*1*). Again no significant changes are found by adding cubic and quartic terms.

The fundamental idea is to compute the energy for a given axis of rotation and a given J by requiring the energy to have a minimum as a function of the centrifugal distortion of the molecular geometry. The moment of inertia and the potential energy are both expressed in terms of a number of independent parameters describing the deformation, and the minimum is easily determined by the computer. Thus, in principle, the classical energy and the corresponding geometry may be computed for any axis of rotation and for any value of J, which means that the complete rotational energy surface may be computed. We have, however, only determined the energy and the corresponding deformations for rotations around the C_4, the C_3, and the C_2 axes. The energy values are the quantities called above E_{max}, E_{min}, and E_{sad}, respectively.

TABLE III

Energy Differences for the Vibrational Ground State

J	$E_{max} - E_{min}$		$E_{sad} - E_{min}$	
	quant. mech.	semi-classical	quant. mech.	semi-classical
20	0.0046	0.0045	0.0034	0.0033
30	0.0231	0.0225	0.018	0.0168
40	0.0724	0.0709	0.055	0.0531
50	0.1754	0.1725	0.136	0.1298
60	0.362	0.358	0.27	0.269
70	0.667	0.657	0.51	0.496

Energy differences are given in cm^{-1}, the number of digits indicating a rough estimate of the accuracy.

The results obtained naturally depend on J, but vary smoothly in a reasonable way. The energy values are all too low, at $J = 70$ by about 10 cm^{-1}, the error being roughly proportional to J. However, when the differences between the energies are formed, amazingly accurate results are obtained, as shown in Table III, where a comparison is made with the results from the quantum mechanical calculations. These calculations do not give any of the values E_{max}, E_{min}, or E_{sad} directly, but E_{max} and E_{min} may be found rather accurately by extrapolating the energy values of each of the two series of clusters by one half-quantum, and the position of E_{sad} may be estimated with reasonable accuracy from an energy level diagram (see Fig. 2 of Ref. (*3*)). The results given in Table III indicate that the semiclassical model in the special case of the vibrational ground state yields accurate energy differences, but it should not be concluded that this model in general is suited for quantitative calculations.

The centrifugal distortion corresponding to a rotation around the C_3 axis is shown in Fig. 11 for $J = 70$. The interesting points are that the centrifugal deformation is

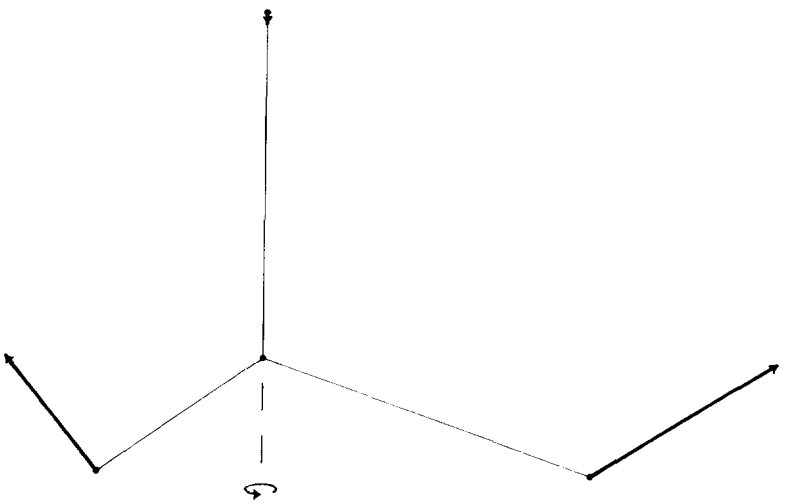

FIG. 11. The computed centrifugal distortion in the vibrational ground state of $^{12}CF_4$ for $J = 70$ due to a rotation around one of the C_3 axes, projected on to one of the FCF-planes, assuming that the C nucleus does not move. The displacements of the nuclei are exaggerated by a factor of 500.

very small and that the movements of the off-axis nuclei are almost as much a stretching of the CF bonds as an angular deformation, contrary to what may falsely be concluded directly from the magnitude of the single constants in the harmonic part of the potential function.

We have tried to make similar calculations for the triply degenerate ν_4 vibrational state, but without success. Once more, this just stresses that the semiclassical model should be used only for qualitative purposes.

CONCLUSION

The semiclassical model is conceptionally very different from the quantum mechanical model. Nevertheless, the two models supplement each other in a very useful way. The quantum mechanical model yields a large number of very accurate data, and the semiclassical model allows an understanding and ordering of these data, apparently without any contradiction between the two models. The present treatment is limited to the isolated vibrational components of CF_4. In a forthcoming paper (*22*) we shall demonstrate that the semiclassical model is able to explain also the structure of the mixing vibrational components.

APPENDIX

The purpose of this appendix is to outline the derivation of an approximate quantization condition that is valid close to the bend of a folded series of clusters, assuming the rotational energy surface to have the form of a perfectly circular ridge or depression centered at a C_4 or a C_3 point. We have to find a quantum mechanical system having the same number of variables and the same form of the energy in the classical limit. A possible choice is a one-dimensional rotor (*24*), describing the rotation of one particle confined to move on a circle. This system has two variables, one in the range 0 to 2π measuring the position of the particle and the other indicating the angular momentum L. The Hamiltonian of this system is

$$H = aL^2, \tag{A1}$$

independent of the position variable. So the form of the energy in the classical limit is a perfectly circular ridge or depression, depending on the sign of the constant a. The energy levels of the one-dimensional rotor are given by

$$E = am^2, \tag{A2}$$

where m is a quantum number having the values $m = 0, \pm1, \pm2, \ldots$.

However, the phase space of the one-dimensional rotor is a cylinder, whereas it is a sphere for the original problem. Consequently, we have to limit the comparison to low values of $|m|$. Also, it might improve the comparison to add a noninteger correction m_0 ($0 \leq m_0 \leq 1$) to m. The cluster index τ of the folded series cannot be identified with the quantum number m, because the start of the series is determined by the part of the rotational energy surface which is inside the circular depression or ridge, but in order that the energy levels should fit near the bend, the difference $\tau - m$ must be a constant integer n.

The quantum condition is consequently

$$E = a(\tau - n + mo)^2. \tag{A3}$$

The energy of the clusters near the bend should thus follow a parabola as a function of the cluster index τ. The presence of the correction m_0 only indicates that the vertex of this parabola does not have to be at an integral value of τ.

ACKNOWLEDGMENT

The stay of B.I.Z. in Aarhus has been financed by the Danish Natural Science Research Council.

RECEIVED: December 29, 1992

REFERENCES

1. S. BRODERSEN, *J. Mol. Spectrosc.* **145,** 331–351 (1991).
2. S. BRODERSEN, to be published.
3. S. G. LARSEN AND S. BRODERSEN, *J. Mol. Spectrosc.* **157,** 220–236 (1993).
4. W. G. HARTER, *Comp. Phys. Rep.* **8,** 319–394 (1988).
5. W. G. HARTER AND C. W. PATTERSON, *J. Chem. Phys.* **80,** 4241–4261 (1984).
6. W. G. HARTER, C. W. PATTERSON, AND J. DAPAIXAO, *Rev. Mod. Phys.* **50,** 37–83 (1978).
7. D. A. SADOVSKII, B. I. ZHILINSKII, J. P. CHAMPION, AND G. PIERRE, *J. Chem. Phys.* **92,** 1523–1537 (1990).
8. V. M. KRIVTSUN, D. A. SADOVSKII, AND B. I. ZHILINSKII, *J. Mol. Spectrosc.* **139,** 126–146 (1990).
9. G. PIERRE, D. A. SADOVSKII, AND B. I. ZHILINSKII, *Europhys. Lett.* **10,** 409–414 (1989).
10. D. A. SADOVSKII AND B. I. ZHILINSKII, *Mol. Phys.* **65,** 109–128 (1988).
11. B. I. ZHILINSKII, "Theory of Complex Molecular Spectra," Chap. 3, Moscow University Press, Moscow, 1989. [in Russian]
12. L. C. BIEDENHARN AND J. D. LOUCK, "Angular Momentum in Quantum Physics, Vol. 8, Encyclopedia of Mathematics" (G. C. Rota, Ed.), Addison-Wesley, Reading, MA, 1981.
13. M. MORSE AND S. S. CAIRNS, "Critical Point Theory and Differential Topology," Academic Press, New York, 1969.
14. A. SOMMERFELD, "Lectures in Theoretical Physics. Mechanics," Vol. 1, Academic Press, New York, 1952.
15. B. I. ZHILINSKII, *Chem. Phys.* **137,** 1–13 (Appendix) (1989).
16. I. M. PAVLICHENKOV AND B. I. ZHILINSKII, *Ann. Phys. (N. Y.)* **184,** 1–32 (1988).
17. J. M. ROBBINS, S. C. CREAGH, AND R. G. LITTLEJOHN, *Phys. Rev. A* **41,** 6052–6062 (1990).
18. W. G. HARTER AND C. W. PATTERSON, *J. Chem. Phys.* **66,** 4872–4885 (1977).
19. B. I. ZHILINSKII, V. I. PEREVALOV, AND V. G. TYUTEREV, "The Irreducible Tensor Operator Method in the Theory of Molecular Spectra," Nauka, Novosibirsk, 1987. [In Russian]
20. W. G. HARTER AND C. W. PATTERSON, *J. Math. Phys.* **20,** 1453–1459 (1979).
21. B. I. ZHILINSKII, unpublished work.
22. S. BRODERSEN AND B. I. ZHILINSKII, to be published.
23. O. I. DAVARASHVILI, B. I. ZHILINSKII, B. M. KRIVTSUN, D. A. SADOVSKII, AND E. P. SNEGIREV, *JETP Lett.* **51,** 18–21 (1990).
24. H. W. KROTO, "Molecular Rotation Spectra," Chap. 9, Wiley, London, 1975.